Applicability analysis of generalized inverse kinematics algorithms with respect to manipulator geometric uncertainties

Yuquan Wang and Lihui Wang

***Abstract*— Accurate kinematic models and measurements are needed in many robotic applications. However uncertainties related to joint angle measurements and manipulator geometry are unavoidable, especially when grasping and using different tools or when we do not have access to an accurate robot model, e.g. when we construct a robotic system by hand. The generalized inverse kinematics methods are not applicable when a manipulator stay inside its singular region. We derive the upper bounds on the joint measurement errors and geometric uncertainties, in order to guarantee that the open-chain serial manipulators stay outside the singular region. These bounds in other words enable en effective execution of generalized inverse kinematics methods for a robotic system which is prone to geometric uncertainties. In addition to the analytic derivation, We validate the proposed bounds through a trajectory tracing task performed by a PR2 robot simulator.**

I. Introduction

Many robotic control applications are based on the generalized inverse kinematics methods, which address the end-effector space error dynamics using joint space variables. This includes the so-called null-space projection based inverse kinematics methods [1] and other methods that are developed upon it, e.g. the stack of tasks [2], and recently the optimization-based algorithms [3]. These computations are however quite sensitive to modeling errors, such as joint angle uncertainties or manipulator geometry inaccuracies.

When robot systems become increasingly complex, the exact geometry, from the robot base to the tip of the tools, inevitably becomes more uncertain. For example from time to time we need to work with tailor made robotic components, e.g. customized tools that are grasped by a robotic gripper or constructing an articulated robotic manipulator from the scratch. There are also cases when an accurate model is not available due to issues regarding intellectual property.

We can address these problems from the control perspectives, such as the adaptive control [4] or the iterative learning control [5]. However these aforementioned methods require a linear or linearizable model, which is not the case for robot models with multiple joints and complex geometry. Furthermore, these approaches cannot handle multiple simultaneous constraints, in the way that a generalized inverse kinematics approach does [1], [2], [3]. In this paper we try to quantitatively address the question of how geometric uncertainties affect the applicability of generalized inverse kinematics algorithms.

Yuquan and Lihui are researchers from Department of Production Engineering, School of Industrial Engineering and Management (ITM) at Royal Institute of Technology (KTH), SE-100 44 Stockholm, Sweden. e-mail: {yuquan}@kth.se

The pseudo-inverse of a manipulator Jacobian is the basis to a series of robotic control methods, e.g. the prioritized tasks approaches [1], [2], [6], the gradient projection approach [7] and the augmented Jacobian approach [8]. The pseudo-inverse can be ill conditioned due to the existence of either kinematic or algorithmic singularities. In this paper we focus on potential kinematic singularities induced by the geometric uncertainties. We define a singular region of a manipulator configuration, which is characterized by the minimum eigenvalue associated with a manipulator Jacobian pseudo inverse, see [9] and [10].

The geometric uncertainties of a manipulator can be categorized as: (1) uncertainties in joint positions, (2) uncertainties in the manipulator geometry. In this paper, we limit ourselves to the open-chain serial manipulators. Basically by deriving bounds on the two kinds of geometric uncertainties, we can guarantee that the manipulator configuration is outside the singular region. If these bounds are fulfilled, we also guarantee the applicability of the generalized inverse kinematic algorithms.

In the first case, we directly derive the bound on the uncertainties of the joint positions using the eigenvalue derivative formula [11] and the closed-form derivative of a manipulator Jacobian. In the second case, we model the geometric uncertainties with virtual joints whose axis are modeled by twist coordinates, see [12]. Using the twist coordinates enables a homogeneous treatment of the virtual joints and the real joints when we derive the manipulator Jacobian. On top of the twist coordinates and thereafter the homogeneous treatment of the virtual and real joint positions, we can derive the bounds in the same way as the in first case.

We use the proposed bounds on a case-by-case basis. As a validation example, we examine the applicability of the generalized inverse kinematics algorithms in case of performing a trajectory tracing task using the 7 degrees of freedom (DOF) arm of a PR2 robot simulator. It shows that if the derived bounds are not met, the manipulator configuration enters the singular region.

The main contribution of this paper is that we propose a way to compute task dependent bounds which capture the applicability of generalized inverse kinematics approaches [1], [2], [6] in the presence of geometric uncertainties.

We organize the rest of the paper as follows: we relate the proposed approach to the state of the art in Sec. II; we introduce the notations and manipulator kinematics in Sec. III; then we mathematically formulate the problem in Sec. IV and derive the bounds on two kinds of geometric uncertainties in Sec. V; the proposed bounds are validated

through simulations in Sec. VI and we conclude the paper in Sec. VII.

II. Related work

Although the null-space projection based inverse kinematics methods [1] have been developed over two decades ago, in many cases we need the assumption that the kinematics is perfectly known. In order to address this problem we can damp or filter the Jacobian [13] or apply more systematic singularity robust redundancy resolution methods, e.g. [9] and [10], that can be applied under kinematic or algorithmic singularities. When a set of linear constraints is used in the inverse kinematic algorithms, the closed-loop stability with respect to (w.r.t.) the interaction between different linear constraints is addressed in [14]. Whereas in the proposed approach we derive bounds on the geometric uncertainties such that the manipulator will not enter the singular region where an inverse kinematics approach is not appropriate to be applied.

The convergence proof of classical inverse kinematics algorithms for redundant robots is reported in [15], where the comparison principle for discrete time systems is used to derive bounds on the gain of the closed-loop inverse kinematics algorithms in relation to the sampling time. When both kinematics and dynamics uncertainties are involved, the stability of feedback control was analyzed in [16] with an Lyapunov approach, where the condition on the perturbed Jacobian matrix is summarized as a bound on the eigenvalue of the product of the manipulator Jacobian matrix and its transpose. However, in this paper, we explicitly model the geometric uncertainties and use the proposed bounds on geometric uncertainties to check if the conditions on the perturbed Jacobian matrix reported by [16] is met.

Virtual mechanisms are widely used in robotics. We can use them to model and estimate the geometric uncertainties in constraint-based programming methods [6] and we can also use virtual mechanisms to model the control variables [6], [17] and [18]. In this paper we use virtual joints to model geometric uncertainties, which enables us to treat the manipulator kinematics and the geometric uncertainties in a unified way through the geometric approach introduced in [12]. In order to keep the consistency, most of the notations are borrowed from [12].

The Bauer-Fike theorem can be used to derive the perturbation of the eigenvalues as in the visual servoing case reported by [19], however the Bauer-Fike theorem is an overestimate and does not give a direction. Assuming that the higher order terms are neglectable, we give a first order approximation of the manipulator Jacobian perturbed by geometric uncertainties using the eigenvalue derivative formula [11]. In cases where it is required to find higher order approximations of the Jacobian, we can use the results in [20].

Alternative to examining the derivative or perturbation of an eigenvalue, *Gershgorin's disc* provides the bound on an eigenvalue using the sum of the elements in the corresponding row. We can find its application in the stability analysis of a formation graph in the context of formation control [21]. However unlike in the case of a formation matrix, a row of the product of a Jacobian matrix and its transpose, does not have an intuitive dependence on the geometric parameters of a manipulator.

If the model equations are well-defined, the *interval analysis*, see [22], provides rigorous bounds on solutions with respect to an interval of inputs. Relying on the forward kinematics mapping, we can use the *interval analysis* to allocate uncertainties on different geometric parameters of a manipulator given the desired end-effector precision [23]. However we cannot find such a clear mapping, e.g. the forward kinematics, between the eigenvalue of the product of a Jacobian matrix and its transpose and the geometric parameters of a manipulator, therefore it is not straightforward to examine the applicability of inverse kinematics algorithms using the interval analysis.

III. Preliminaries

We first list the notations to be used throughout the paper and introduce the kinematics of a manipulator to facilitate the further discussion.

A. Notation

- $\boldsymbol{\xi} \in \mathbb{R}^{6\times 1}$ a twist coordinate corresponding to an axis of a real joint of a robotic manipulator.
- $\boldsymbol{\theta} \in \mathbb{R}^{n\times 1}$ - joint positions of a manipulator, where n denotes the number of DOF. We use θ_i to denote the ith joint position.
- $\vee$(vee) and $\wedge$(wedge) operator. We obtain the twist: $\hat{\boldsymbol{\xi}} \in se(3)$ associated with a twist coordinate by using the $\wedge$(wedge) operator and vice versa we can obtain the twist coordinate from a twist with the $\vee$(vee) operator.
- $\boldsymbol{\chi}_{i,j} \in \mathbb{R}^{6\times 1}$ a twist coordinate corresponding to the axis of the jth virtual joint, which is between the ith and $i+1$th joint of the nominal kinematic chain.
- $\alpha_{i,j}$, the uncertainty joint position associated with the twist coordinate $\boldsymbol{\chi}_{i,j}$.
- $R \in SO(3)$, a rotation matrix.
- $\boldsymbol{t} \in \mathbb{R}^3$ - a translation.
- $g : \mathbb{R}^4 \to \mathbb{R}^4$ - a homogeneous transformation, where $g = (\boldsymbol{t}, R) \in SE(3)$. $g_{i-1,i}$ defines the Euclidean transformation of frame i w.r.t. frame $i-1$.
- $Ad_g : \mathbb{R}^6 \to \mathbb{R}^6$ - an adjoint transformation. Given $g = (\boldsymbol{t}, R) \in SE(3)$, Ad_g and its inverse are:

$$Ad_g = \begin{bmatrix} R & \hat{\boldsymbol{t}}R \\ O & R \end{bmatrix}, \quad Ad_g^{-1} = \begin{bmatrix} R^\top & -R^\top\hat{\boldsymbol{t}} \\ O & R^\top \end{bmatrix}.$$

- J - a Jacobian matrix. We use $\tilde{J}$ to denote the Jacobian perturbed by geometric uncertainties.

B. Manipulator Kinematics

According to the Chasles' theorem, we know that every rigid motion can be realized as a screw motion and we can use the exponential map to generate a screw motion from a twist as: $e^{\hat{\boldsymbol{\xi}}\theta} \in SE(3)$, see [12]. In light of the

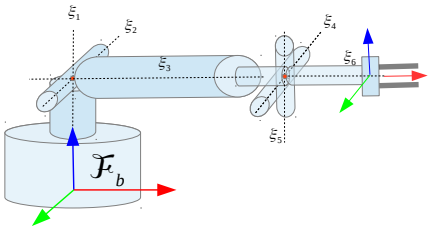

Fig. 1: A schematic view of the manipulator kinematics, where the manipulator is at its initial configuration, i.e. $\boldsymbol{\theta} = \mathbf{0}$. The axis of each joint is labeled by the corresponding twist coordinates $\boldsymbol{\xi}_i$ for $i = 1, \ldots, 6$.

aforementioned facts, we can use the parameterizable screw motion to formulate the manipulator kinematics.

In Fig. 1 and 2, we can find a schematic view of the forward kinematics of an open-chain serial manipulator. From the base to the end-effector, we number the links from 0 to n and joint i connects link $i-1$ and link i. If we assign each link a link frame and denote the transformation between the adjacent link frames as $g_{i-1,i}(\theta_i)$, the overall forward kinematics is given by:

$$g_{0n}(\boldsymbol{\theta}) = g_{0,1}(\theta_1) g_{1,2}(\theta_2) \ldots g_{n-1,n}(\theta_n). \tag{1}$$

In Fig. 1, we depict the kinematics of a manipulator at its initial configuration. We denote the initial Euclidean transformation of frame $\mathcal{F}_e$ w.r.t. the base frame $\mathcal{F}_b$ as $g_{be}(\mathbf{0})$. We specify the joint axis with the twist coordinate $\boldsymbol{\xi}_i$ for $i = 1, \ldots, 6$. These twists are constant twists obtained by evaluating the screw motion when $\boldsymbol{\theta} = \mathbf{0}$ in the base frame $\mathcal{F}_b$.

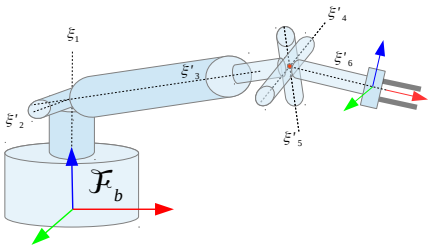

Fig. 2: The schematic view of the manipulator kinematics when $\boldsymbol{\theta} \neq \mathbf{0}$. For this manipulator as we choose $\boldsymbol{\xi}_1$ to be parallel with the z axis of $\mathcal{F}_b$, $\boldsymbol{\xi}_1$ does not change when $\boldsymbol{\theta} \neq \mathbf{0}$, however in this case the new twist coordinates $\boldsymbol{\xi}'_i$ for $i = 2, \ldots, n$ are given by (3).

In case of Fig. 2, the manipulator is away from its initial configuration, i.e. $\boldsymbol{\theta} \neq \mathbf{0}$. As we can use the exponential of a twist to represent the relative motion of the corresponding joint with respect to its initial position, see [12], then we can express the forward kinematics (1) with the *product of exponentials formula* (POE) [24]:

$$g_{0,n} = e^{\hat{\boldsymbol{\xi}}_1 \theta_1} e^{\hat{\boldsymbol{\xi}'}_2 \theta_2} \ldots e^{\hat{\boldsymbol{\xi}'}_n \theta_n} g_{0,n}(\mathbf{0}), \tag{2}$$

where we denote the new twist coordinate for $i = 2 \ldots n$ as:

$$\boldsymbol{\xi}'_i = \left(\frac{\partial g}{\partial \theta_i} g^{-1} \right)^{\vee} = Ad_{g_{1,i-1}} \boldsymbol{\xi}_i. \tag{3}$$

Using the property of the adjoint transformation, we know that $Ad_{g_{1,i-1}} \boldsymbol{\xi}_i$ corresponds to the twist $g_{1,i-1} \hat{\boldsymbol{\xi}}_i g_{1,i-1}^{-1}$.

C. Differential Kinematics

For a general mapping $g(\boldsymbol{\theta}) \in SE(3)$, its derivative $\dot{g}(\boldsymbol{\theta}) \notin se(3)$. Rather, we have the instantaneous spatial velocity given by $\frac{\partial g}{\partial \boldsymbol{\theta}} g^{-1} \in se(3)$, where we suppress the explicit dependence on $\boldsymbol{\theta}$ for notation compactness. Let us expand $\frac{\partial g}{\partial \boldsymbol{\theta}} g^{-1}$ as: $\sum_{i=1}^{n} \left(\frac{\partial g}{\partial \theta_i} g^{-1} \right) \dot{\theta}_i$. Since $\frac{\partial g}{\partial \theta_i} g^{-1}$ are matrix evaluated, we use the twist coordinate (3) to put them into a compact form, see [12], as:

$$\boldsymbol{V} = J \dot{\boldsymbol{\theta}} = [\boldsymbol{\xi}_1, \boldsymbol{\xi}'_2 \ldots, \boldsymbol{\xi}'_n] \dot{\boldsymbol{\theta}}. \tag{4}$$

IV. Problem Formulation

In order to derive the dependency of the singularity of a robot manipulator with respect to the geometric uncertainties, we introduce the singular region of a manipulator configuration. We characterize the geometric uncertainties associated with a manipulator from two perspectives and then mathematically formulate the problem of bounding the geometric uncertainties such that the manipulator configuration is outside the singular region.

As reported in [9] and [10], the robustness of inverse kinematics algorithms depends on the eigenvalues of the product of the manipulator Jacobian matrix and its transpose. If there are near zero singular values, the manipulator needs to generate un-affordable large joint velocities to fulfill task space requirements. In the vicinity of a singular configuration, we define a singular region of a manipulator by constraining the minimum eigenvalue λ_{min} with a pre-specified threshold λ_0 as:

Definition 1 (Singular region of a manipulator): We use the smallest eigenvalue λ_{min} of $JJ^{\top}$ and a pre-specified threshold λ_0 to define a singular region as:

$$\mathcal{D} = \{ \boldsymbol{\theta} \mid 0 \leq \lambda_{min} < \lambda_0 \}. \tag{5}$$

Within the singular region of a manipulator, the inverse kinematics is ill-conditioned. ■

We group the geometric uncertainties of a manipulator into two classes: (1) uncertainties of the joint positions: $\delta\boldsymbol{\theta}$, see Fig. 3 (2) uncertainties of the manipulator geometry, see Fig. 4. In the first case, we assume that the geometry of the manipulator is perfectly known, whereas $\boldsymbol{\theta}$ is not accurately measured. More than a complement to the first case, uncertainties are more likely to be associated with the manipulator geometry. In this case we can model the geometric uncertainties δg_i between link i and link $i+1$ of the manipulator with at most 6 virtual joints. Namely in the forward kinematics (2) of a manipulator, we use $e^{\hat{\boldsymbol{\xi}}'_i \theta_i} \delta g_i e^{\hat{\boldsymbol{\xi}}'_{i+1} \theta_{i+1}}$ instead of $e^{\hat{\boldsymbol{\xi}}'_i \theta_i} e^{\hat{\boldsymbol{\xi}}'_{i+1} \theta_{i+1}}$.

As a zero pitch screw corresponds to a revolute joint and an infinite pitch screw corresponds to a prismatic joint. We can select a specific combination of virtual joints to form a virtual kinematic chain to model different sorts of geometric uncertainties. We use $\boldsymbol{\chi}_{i,j}$ for $j = 1, \ldots, 6$ to denote the twist coordinates associated with the joints of the uncertainty kinematic chain and use $\alpha_{i,j}$ for $j = 1, \ldots, 6$ to denote the associated uncertainty joint positions.

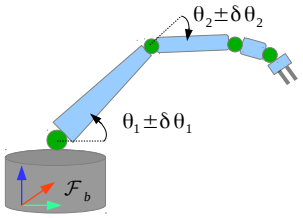

Fig. 3: Potential joint position uncertainties $\delta\theta_i$ of a serial manipulator.

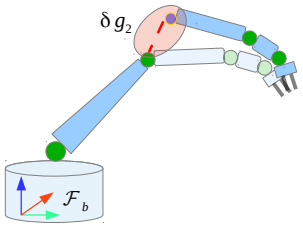

Fig. 4: The manipulator geometry might not be perfectly modeled. In this example, we can see that the second link is mis-aligned from its nominal position by δg_2.

In view of the product of exponentials formula (2) and the twist coordinates $\boldsymbol{\chi}_{i,j}$ for $j = 1 \dots 6$, we can express the forward kinematics of the uncertainty kinematic chain as:

$$\delta g_i = e^{\hat{\boldsymbol{\chi}}_{i,1}\alpha_{i,1}} e^{\hat{\boldsymbol{\chi}}_{i,2}\alpha_{i,2}} \dots e^{\hat{\boldsymbol{\chi}}_{i,6}\alpha_{i,6}} \delta g_i(\mathbf{0}). \tag{6}$$

As (6) only affects the twist coordinates $\boldsymbol{\xi}'_k$, for $k \geq i+1$, of the manipulator Jacobian (4), we define the perturbed manipulator Jacobian as:

$$\tilde{J} = [\boldsymbol{\xi}'_1, \boldsymbol{\xi}'_2 \dots, \boldsymbol{\xi}'_i, \tilde{\boldsymbol{\xi}}'_{i+1}, \tilde{\boldsymbol{\xi}}'_{i+2}, \dots, \tilde{\boldsymbol{\xi}}'_n], \tag{7}$$

where $\boldsymbol{\xi}'_i$ is defined in (3) and $\tilde{\boldsymbol{\xi}}'_{i+1}$ is defined as:

$$\tilde{\boldsymbol{\xi}}'_{i+1} = \left(\frac{\partial g}{\partial \theta_{i+1}} g^{-1}\right)^{\vee} = Ad_{g_{1,i}} Ad_{\delta g_i} Ad_{g_{i,i+1}} \boldsymbol{\xi}_{i+1}. \tag{8}$$

Using the definitions of the singular region and the forward kinematics of the uncertainty kinematic chain, we summarize the dependency of the singularity of a robot manipulator with respect to the geometric uncertainties as the following two problems:

Problem 1: Suppose there are uncertainties associated with the joint positions $|\delta\theta_i|$ for $i = 1, 2, \dots, n$, we derive bounds on joint positions: $|\delta\theta_i| < \gamma_{\theta_i}$ for $i = 1, 2, \dots, n$, such that the manipulator configuration w.r.t. to Jacobian (4) is outside the singular region $\mathcal{D}$ that is defined in (5). Thereby the derived bounds enable the use of general inverse kinematics approaches [1], [2], [6]. ■

Problem 2: Assuming that there exists geometric uncertainty between the ith and $i+1$th link of a manipulator, we model the geometric uncertainty with a uncertainty kinematic chain with at most 6DOF, which can be specified by twist coordinates and uncertainty joint positions $\boldsymbol{\chi}_{i,j}$ and $\alpha_{i,j}$ for $j = 1, \dots, 6$.

We derive bounds on uncertainty joint positions: $|\delta\alpha_{i,j}| < \gamma_{\alpha_{i,j}}$ for $j = 1, 2, \dots, 6$, such that the manipulator configuration w.r.t. Jacobian (7) is outside the singular region $\mathcal{D}$ that is defined in (5). Thereby the derived bounds enable the use of general inverse kinematics approaches [1], [2], [6]. ■

V. Proposed Solution

We separate the solution to Problem 1 and Problem 2 in Theorem 1 and 2 respectively. In Theorem 1, we assume that the kinematics of the manipulator is known and derive a bound on $\delta\boldsymbol{\theta}$. Then in Theorem 2, we likewise assume that the joint positions $\boldsymbol{\theta}$ are correctly measured and derive bounds on the uncertainties $\delta\boldsymbol{\alpha}_i$.

Remark 5.1: Note that in Problem 2 we only consider the case when one uncertainty kinematic chain is used. However, based on the manipulator Jacobian derivation, i.e. (2-4), and the homogeneous treatment of virtual and real twist coordinates, i.e. (6-8), we know that Problem 2 can be extended to the case when multiple uncertainty kinematic chains are involved in the same manipulator. Basically we only need to use several virtual kinematic chains which are modeled by (6) in the development of the perturbed manipulator Jacobian (7).

In view of clarity and simplified computation, we separate the discussion of the meta cases in Problem 1 and 2 respectively. ■

Theorem 1: Assume that the manipulator is outside the singular region (5) initially and that the second order terms can be neglected. While executing a certain task at time step k, if the bound $\gamma_{\theta_j}(k)$ on the joint position uncertainty $\delta\theta_j$ fulfills:

$$|\delta\theta_j| < \gamma_{\theta_j}(k) = |\frac{\lambda_0 - \lambda_{min}(k)}{\lambda'_j}|, \tag{9}$$

then the manipulator configuration is outside the singular region $\mathcal{D}$. The partial derivative λ'_j in (9) is defined as:

$$\lambda'_j = \frac{\partial \lambda_{min}}{\partial \theta_j} = \boldsymbol{x}_{min}^{\top}[\frac{\partial J}{\partial \theta_j} J^{\top} + J(\frac{\partial J}{\partial \theta_j})^{\top}]\boldsymbol{x}_{min},$$

where $\boldsymbol{x}_{min}^{\top}$ denotes the eigenvector of $JJ^{\top}$ associated with $\lambda_{min}(k)$ and we have the closed-form derivative $\frac{\partial J}{\partial \theta_j} \in \mathbb{R}^{6\times n}$ for $j = 1, \dots, n$ in (12).

Proof: We need to constrain $\delta\theta_j$ using the condition: $\lambda_{min}(k+1) > \lambda_0$, which indicates that the manipulator is out of the singular region (5). If we remove higher order terms we get the approximation

$$\lambda_{min}(k+1) = \lambda_{min}(k) + \frac{\partial \lambda_{min}(k)}{\partial \theta_j}\delta\theta_j,$$

which together with the aforementioned condition on θ_j gives:

$$\lambda_{min}(k) + \frac{\partial \lambda_{min}(k)}{\partial \theta_j}\delta\theta_j > \lambda_0.$$

Thus, if we denote $\lambda'_j = \frac{\partial \lambda_{min}(k)}{\partial \theta_j}$, we have:

$$\begin{cases} \delta\theta_j > \underbrace{\dfrac{\lambda_0 - \lambda_{min}(k)}{\lambda'_j}}_{<0}, & \text{if } \lambda'_j > 0, \\ \delta\theta_j < \underbrace{\dfrac{\lambda_0 - \lambda_{min}(k)}{\lambda'_j}}_{>0}, & \text{if } \lambda'_j < 0. \end{cases}$$

or equivalently:

$$|\delta\theta_j| < |\frac{\lambda_0 - \lambda_{min}(k)}{\lambda'_j}|. \tag{10}$$

Applying the method reported in [11], the derivative of an eigenvalue $\dot{\lambda}$ of a matrix A can be computed as: $\dot{\lambda} = \boldsymbol{y}^\top \dot{A} \boldsymbol{x}$, where $\boldsymbol{x}, \boldsymbol{y}$ denote the right and left eigenvector respectively. In light of this we can calculate λ'_j as:

$$\begin{aligned}\lambda'_j &= \frac{\partial \lambda_{min}(k)}{\partial \theta_j} = \boldsymbol{y}_{min}^\top \frac{\partial JJ^\top}{\partial \theta_j} \boldsymbol{x}_{min} = \boldsymbol{x}_{min}^\top \frac{\partial JJ^\top}{\partial \theta_j} \boldsymbol{x}_{min} \\ &= \boldsymbol{x}_{min}^\top [\frac{\partial J}{\partial \theta_j} J^\top + J(\frac{\partial J}{\partial \theta_j})^\top] \boldsymbol{x}_{min}\end{aligned} \tag{11}$$

where we used the fact that $JJ^\top$ is a real and symmetric matrix such that the left eigenvector $\boldsymbol{y}_{min}^T$ is identical to the right eigenvector $\boldsymbol{x}_{min}^T$ and then using Lemma 1, we have the closed-form derivative $\frac{\partial J}{\partial \theta_j} \in \mathbb{R}^{6\times n}$ for $j = 1, \ldots, n$ as:

$$\frac{\partial J}{\partial \theta_j} = [\frac{\partial \boldsymbol{\xi}'_1}{\partial \theta_j} \ \frac{\partial \boldsymbol{\xi}'_2}{\partial \theta_j} \cdots \ \frac{\partial \boldsymbol{\xi}'_n}{\partial \theta_j}]. \tag{12}$$

Then using condition (10) and the partial derivative expression (11), we can conclude the bound (9). ■

Lemma 1: For each column of the Jacobian (4), we have

$$\frac{\partial}{\partial \theta_j} \boldsymbol{\xi}'_i = \begin{cases} [\boldsymbol{\xi}'_j \ \boldsymbol{\xi}'_i], & j \le i \le n \\ \mathbf{0} & i < j \le n \end{cases}, \tag{13}$$

where we separate the twist coordinate $\boldsymbol{\xi} = [\boldsymbol{\nu}^T, \boldsymbol{\omega}^T]^T$ with $\boldsymbol{\nu}, \boldsymbol{\omega} \in \mathcal{R}^{3\times 1}$ and we have the Lie bracket $[\boldsymbol{\xi}'_j \ \boldsymbol{\xi}'_i] = (\boldsymbol{\omega}_j \times \boldsymbol{\nu}_i - \boldsymbol{\nu}_j \times \boldsymbol{\omega}_i, \boldsymbol{\omega}_j \times \boldsymbol{\omega}_i)$.

Proof: See appendix I. ■

Theorem 2: Assume that the manipulator is outside the singular region (5) initially and that second order terms can be neglected. We model the geometric uncertainty between the ith and $i+1$th link of a manipulator with twist coordinates $\boldsymbol{\chi}_{i,j}$ and uncertainty joint positions $\alpha_{i,j}$ for $j = 1, \ldots, 6$. While executing a certain task we assume that the joint positions are always correctly measured, i.e. $\delta\boldsymbol{\theta} = \mathbf{0}$, and the uncertainty joint position $\alpha_{i,j}$ for $j = 1, \ldots, 6$ are static.

At time step k, if the bound $\gamma_{\alpha_{i,j}}(k)$ on an uncertainty position $\alpha_{i,j}$ fulfills:

$$|\alpha_{i,j}| < \gamma_{\alpha_{i,j}}(k) = |\frac{\lambda_0 - \tilde{\lambda}_{min}(k)}{\tilde{\lambda}'_j}|, \tag{14}$$

then the manipulator configuration is outside the singular region (5). The partial derivative $\tilde{\lambda}'_j$ in (14) is defined as:

$$\tilde{\lambda}'_j = \frac{\partial \tilde{\lambda}_{min}}{\partial \alpha_{i,j}} = \tilde{\boldsymbol{x}}_{min}^\top [\frac{\partial \tilde{J}}{\partial \alpha_{i,j}} \tilde{J}^\top + \tilde{J}(\frac{\partial \tilde{J}}{\partial \alpha_{i,j}})^\top] \tilde{\boldsymbol{x}}_{min},$$

where $\tilde{\boldsymbol{x}}_{min}$ denotes the eigenvector of $\tilde{J}\tilde{J}^\top$ associated with $\tilde{\lambda}_{min}$ and $\frac{\partial \tilde{J}}{\partial \alpha_{i,j}}$ is given in (15).

Proof: Following the proof of Theorem 1, it is straightforward to prove Theorem 2 except the calculation of $\frac{\partial \tilde{J}}{\partial \alpha_{i,j}}$. Compare the affected Jacobian $\tilde{J}$ given in (7) with the nominal Jacobian J given in (4), we can find that the difference is due to the twist coordinates $\tilde{\boldsymbol{\xi}}'_k$ for $k = i+1, \ldots, n$ given in (8) that are affected by the uncertain geometry $\delta g_{i,6}$. Using this fact, we can conclude the structure of $\frac{\partial \tilde{J}}{\partial \alpha_{i,j}}$ fulfills:

$$\frac{\partial \tilde{J}}{\partial \alpha_{i,j}} = [\mathbf{0}, \ \ldots, \mathbf{0}, \ \frac{\partial \boldsymbol{\xi}'_{i+1}}{\partial \alpha_{i,j}} \ \frac{\partial \boldsymbol{\xi}'_{i+2}}{\partial \alpha_{i,j}} \ \ldots, \ \frac{\partial \boldsymbol{\xi}'_n}{\partial \alpha_{i,j}}], \tag{15}$$

where we used the fact that $\frac{\partial \boldsymbol{\xi}'_k}{\partial \alpha_{i,j}} = \mathbf{0}$ for $k = 1, \ldots, i$ as every $\boldsymbol{\xi}'_k$, that is given in (3), is not affected by $\delta g_{i,6}$. In order to calculate $\frac{\partial \tilde{\boldsymbol{\xi}}'_{i+1}}{\partial \alpha_{i,j}}$ using the development of $\frac{\partial \boldsymbol{\xi}'_i}{\partial q_j}$, we define an augmented set of twist coordinates:

$$[\boldsymbol{\xi}_1, \boldsymbol{\xi}_2 \ldots, \boldsymbol{\xi}_i, \boldsymbol{\chi}_{i,1}, \boldsymbol{\chi}_{i,2}, \ldots, \boldsymbol{\chi}_{i,6}, \boldsymbol{\xi}_{i+1}, \ldots, \boldsymbol{\xi}_n]. \tag{16}$$

Then we can conclude that when $k = i+1, \ldots, n$,

$$\frac{\partial}{\partial \alpha_{i,j}} \hat{\boldsymbol{\xi}}_k = \hat{\boldsymbol{\chi}}'_{i,j} \hat{\boldsymbol{\xi}}'_k - \hat{\boldsymbol{\xi}}'_k \hat{\boldsymbol{\chi}}'_{i,j} = [\hat{\boldsymbol{\chi}}'_{i,j} \ \ \hat{\boldsymbol{\xi}}'_k],$$

where $\boldsymbol{\xi}'_k$ is given in (8) and $\boldsymbol{\chi}'_{i,j}$ is defined as:

$$\boldsymbol{\chi}'_{i,j} = \left(\frac{\partial g}{\partial \alpha_{i,j}} g^{-1}\right)^\vee = Ad_{g_{1,i}} Ad_{\delta g_{i,j}} \boldsymbol{\chi}_{i,j}.$$

■

Remark 5.2: As we use the derivative of $\tilde{J}$ to infer the bounds on $\boldsymbol{\alpha}_i$, we choose the origin of $\boldsymbol{\alpha}_i$ as the equilibrium to simplify the calculation, i.e. $\delta g_{i,j} = I$ when $\boldsymbol{\alpha}_i = \mathbf{0}$. In case that we need to choose values other than the origin, we would have a non-identity yet static $\delta g_{i,j}$ when calculating the new twist coordinate $\boldsymbol{\chi}'_{i,j}$. ■

VI. Simulation verification

In this section we verify the bounds $\gamma_{\theta_j}(k)$ and $\gamma_{\alpha_{ij}}(k)$ that are proposed in Theorem 1 and 2 respectively through simulations[1] . The kinematics of the PR2 robot is well modeled in ROS, which provides us a good basis to analyze the worst case geometric uncertainties using the proposed theorems. We use the left arm of the PR2 robot simulator,[2] which has 7 DOF, and a sample trajectory tracing task to examine the bounds (9) and (14) which are both task and manipulator configuration dependent. The kinematics of the robot arm is shown in Fig. 5 and the trajectory is shown in Fig. 6. From the simulation results, we conclude that if the bounds were not met the manipulator configuration would enter the singular region.

We use a variation of constraint based programming [3] to formulate a quadratic optimization problem that includes the minimization of joint velocities, joint limits and a translation constraint:

$$J\dot{\boldsymbol{\theta}} = -k\Delta\boldsymbol{d} \tag{17}$$

where only the translational part of J is used, $\Delta\boldsymbol{d}$ denotes the difference between the end effector position and the desired position and k denotes a gain. In the translation task (17), the desired trajectory is a Lissajous curve, which is shown in Fig. 6. The forward kinematics and Jacobians are calculated using the *Orocos kinematics and dynamics*

[1]Details about the calculation of $\gamma_{\theta_j}(k)$ and $\gamma_{\alpha_{ij}}(k)$ are available at the Git repor: https://github.com/wyqsndd/singularityAnalysis

[2]We use the simulator within ROS Indigo: http://wiki.ros.org/indigo

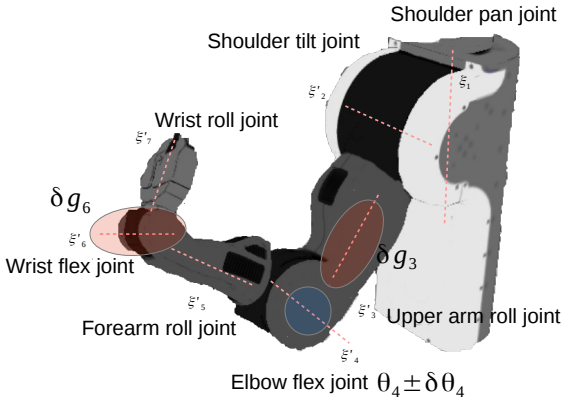

Fig. 5: A schematic view of the kinematics of the left arm of the PR2 robot.

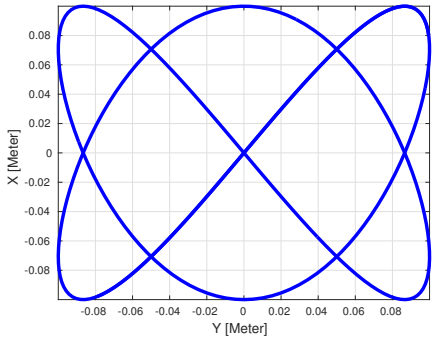

Fig. 6: A Lissajous curve that is traced by the left manipulator of the PR2 robot, where all 7DOF of the arm are used. The robot arm is constrained in three aspects, joint limits, minimization of joint velocities and the constraint (17). We use this example to test both the task and manipulator configuration dependent bounds (9) and (14) that are proposed in Theorem 1 and 2 respectively.

library[3]. We specify the singular region (5) of the left arm by choosing the threshold $\lambda_0 = 0.01$.

We validate Theorem 1 and 2 separately in section VI-A and VI-B. In both cases, we first identify where the geometric uncertainties have the most impact on the minimum eigenvalue λ_{min}, then we add offsets to the corresponding joint position or manipulator geometry to examine the validity of the corresponding bounds.

From these two sets of simulations, we can conclude that if we had a tailor made robotic manipulator, the worst joint uncertainty, w.r.t. this curve tracing task, we can bear at the elbow-flex joint is 0.085 radians and the worst translation offset along the x axis between the third and the forth link is $7.4cm$.

A. *Joint position uncertainties*

In case of Theorem 1, we assume that the kinematics of the manipulator is perfectly known and we need to examine the bounds γ_{θ_j} on $\delta\theta_j$. As stated in (9), the bound $\gamma_{\theta_j}(k)$ depends on the partial derivative $\lambda'_j = \boldsymbol{x}_{min}^\top \frac{\partial JJ^\top}{\partial \theta_j} \boldsymbol{x}_{min}$. In Fig. 7, we plot λ'_j corresponding to θ_j, for $j = 1, \ldots, 7$.

Using the simulated λ'_j and equation (9), we can obtain the corresponding $\gamma_{\theta_j}(k)$ for all the joints at each time step

[3]http://www.orocos.org/kdl

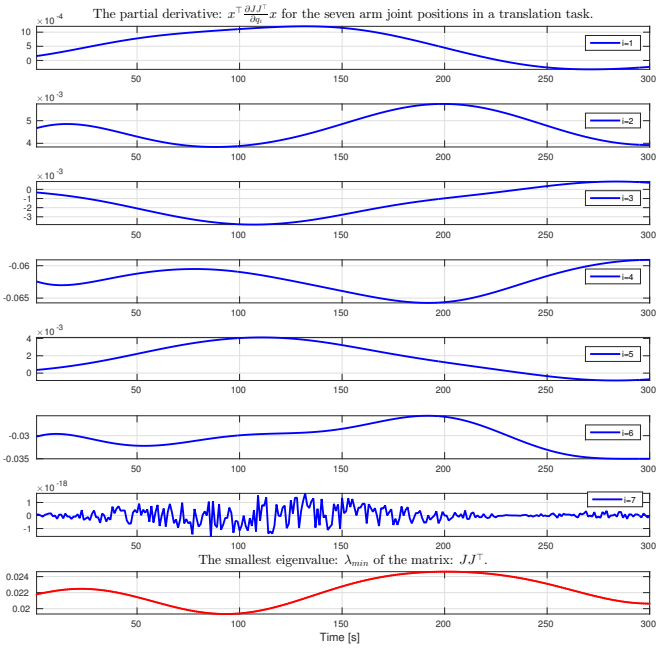

Fig. 7: The partial derivative λ'_j for each joint of the manipulator.

as shown in Fig. 8. Note that we did not calculate $\gamma_{\theta_7}(k)$ due to the fact that λ'_7 shown in the last row of Fig. 7 is close to zero.

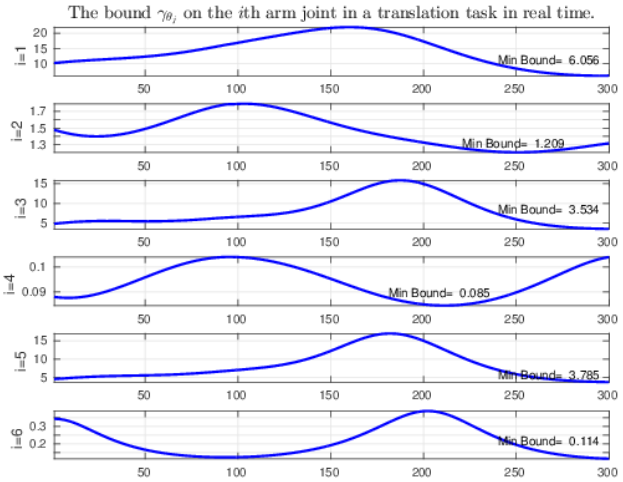

Fig. 8: The bound γ_{θ_j} for each joint according to Theorem 1.

From Fig. 7 we can see that the 4th and 6th joints, which are the elbow-flex and wrist-flex joints, have a relatively larger impact on λ_{min}. From Fig. 8, we can find the minimum $\gamma_{\theta_4} = 0.085$ and $\gamma_{\theta_4} = 0.114$ radians. Therefore we choose to add an offset to the elbow-flex joint to disturb λ_{min}.

If we break the bound $\gamma_{\theta_4} = 0.085$ by adding a constant offset $\delta\theta_4 = 0.1$ radians to θ_4, then in Fig. 9 we can see that in the same task, the manipulator will enter the singular region as we expected according to Theorem 1.

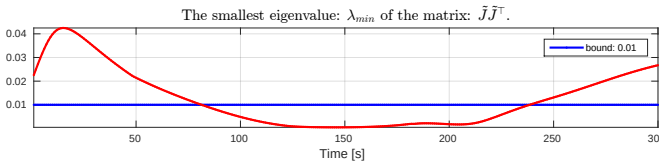

Fig. 9: We can find that the perturbed λ_{min} is lower than the bound $\lambda_0 = 0.01$ that defines the singularity region.

B. Manipulator geometric uncertainties

Then we move on to verify the bounds on the geometric uncertainties which are proposed in Theorem 2. As afore-

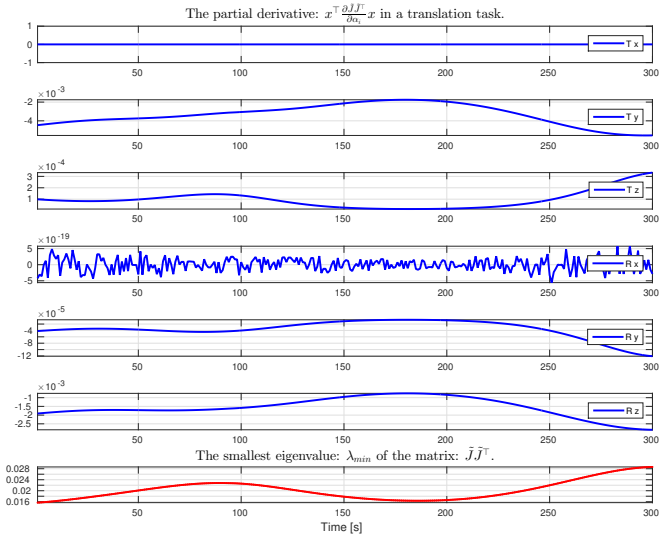

Fig. 10: In this example, we choose to place the geometric uncertainties between the sixth and seventh link of the nominal manipulator. The 6DOF uncertainty kinematic chain models the translation and rotation along x, y and z axis. We plot the partial derivative $\tilde{\lambda}'_j = \boldsymbol{x}_{min}^\top \frac{\partial \tilde{J}\tilde{J}^\top}{\partial \alpha_{6,j}} \boldsymbol{x}_{min}$ for each uncertainty joint position $\alpha_{6,j}$ for $j = 1, \ldots, 6$ of the manipulator.

mentioned in the last section, from Fig. 7, we can see that the impact on λ_{min} varies w.r.t. where we place the joint position uncertainties. If we place the uncertainty kinematic chain at the end of the manipulator where λ'_7 is relatively small, i.e. δg_6 between the wrist-flex and wrist-roll joints shown in Fig. 5, we would expect a small impact on $\tilde{\lambda}_{min}$. This hypothesis is verified by Fig. 10, where we plot the partial derivatives $\tilde{\lambda}'_j =$ for $j = 1, \ldots, 6$ and we can find $\tilde{\lambda}'_j$ are all close or equal to zero.

In order to demonstrate the perturbation on $\tilde{\lambda}_{min}$, we choose to place the geometric uncertainties between the third and forth link of the manipulator, i.e. δg_3 between the upper-arm-roll joint and the elbow-flex joint. According to the simulated partial derivatives: $\tilde{\lambda}'_j$ shown in Fig. 11, we use the larger derivatives $\tilde{\lambda}'_j$ for $j = 1, 3$. Using equation (14), we plot the bound $\gamma_{\alpha_{3,i}}$ for $i = 1, 3$ in Fig. 12. We can tell that the bottle-neck is $\gamma_{\alpha_{3,1}} = 7.4cm$. If we choose to add constant disturbance $\alpha_{3,1} = 10cm$, we find that the manipulator configuration enters the singular region as shown in Fig. 13.

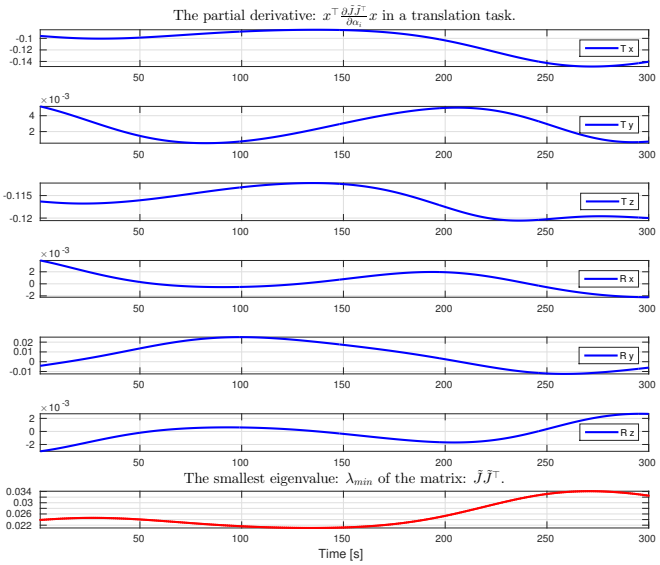

Fig. 11: In this example, we choose to place the geometric uncertainties between the third and forth link of the nominal manipulator. We plot the partial derivative $\tilde{\lambda}'_3 = \boldsymbol{x}_{min}^\top \frac{\partial \tilde{J}\tilde{J}^\top}{\partial \alpha_{3,j}} \boldsymbol{x}_{min}$ for each uncertainty joint position $\alpha_{3,j}$ for $j = 1, \ldots, 6$.

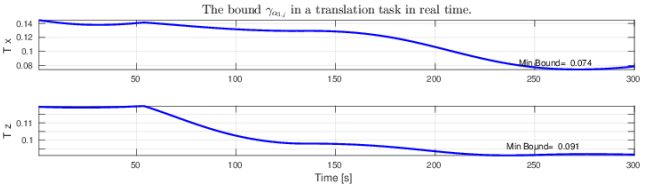

Fig. 12: The bound $\alpha_{3,j}$ for $j = 1, 3$ according to Theorem 2.

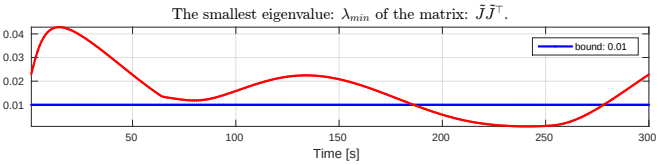

Fig. 13: We can find that the perturbed $\tilde{\lambda}_{min}$ is lower than the bound $\lambda_0 = 0.01$ that defines the singularity region.

VII. Conclusions

The geometric uncertainties arise in robotic kinematics when we work with tailor made robotic components or systems. These uncertainties challenge the applicability of the generalized inverse kinematics algorithms [1], [2], [6]. In order to keep the manipulator configuration outside a singular region, we derive the bounds on two kinds of geometric uncertainties of a manipulator in Theorem 1 and 2. The proposed bounds are both task and manipulator configuration dependent. We verify the validity of these bounds through simulations performed on a PR2 robot simulator in a translation task.

APPENDIX I
PROOF OF LEMMA 1

In case that $i < j$, using (3) we know that $\boldsymbol{\xi}_i'$ is not a function of q_j, otherwise:

$$\frac{\partial}{\partial\theta_j}\hat{\boldsymbol{\xi}}_i' = \frac{\partial g_{1,i-1}}{\partial\theta_j}\hat{\boldsymbol{\xi}}_i g_{1,i-1}^{-1} + g_{1,i-1}\hat{\boldsymbol{\xi}}_i\frac{\partial g_{1,i-1}^{-1}}{\partial\theta_j} \tag{18}$$

where we have

$$\begin{aligned}\frac{\partial g_{1,i-1}}{\partial\theta_j} &= e^{\hat{\boldsymbol{\xi}}_1\theta_1}\dots\hat{\boldsymbol{\xi}}_j e^{\hat{\boldsymbol{\xi}}_j\theta_j}\dots e^{\hat{\boldsymbol{\xi}}_{i-1}\theta_{i-1}} \\ &= \hat{\boldsymbol{\xi}}_j' g_{1,i-1}\end{aligned} \tag{19}$$

$$\begin{aligned}\frac{\partial g_{1,i-1}^{-1}}{\partial\theta_j} &= -e^{-\hat{\boldsymbol{\xi}}_{i-1}\theta_{i-1}}\dots\hat{\boldsymbol{\xi}}_j e^{-\hat{\boldsymbol{\xi}}_j\theta_j}\dots e^{-\hat{\boldsymbol{\xi}}_1\theta_1} \\ &= -e^{-\hat{\boldsymbol{\xi}}_{i-1}\theta_{i-1}}\dots\hat{\boldsymbol{\xi}}_j e^{-\hat{\boldsymbol{\xi}}_j\theta_j}\dots e^{-\hat{\boldsymbol{\xi}}_1\theta_1} \\ &= -e^{-\hat{\boldsymbol{\xi}}_{i-1}\theta_{i-1}}\dots e^{-\hat{\boldsymbol{\xi}}_j\hat{\boldsymbol{\xi}}\theta_j\hat{\boldsymbol{\xi}}_j^{-1}}\hat{\boldsymbol{\xi}}_j\dots e^{-\hat{\boldsymbol{\xi}}_1\theta_1} \\ &= -g_{1,i-1}^{-1}\hat{\boldsymbol{\xi}}_j'\end{aligned} \tag{20}$$

where we used the fact that $g^{-1}e^{\hat{\boldsymbol{\xi}}\theta}g = e^{g^{-1}\hat{\boldsymbol{\xi}}\theta g}$. Plug (19) and (20) into (18), we obtain:

$$\begin{aligned}\frac{\partial}{\partial\theta_j}\hat{\boldsymbol{\xi}}_i &= \hat{\boldsymbol{\xi}}_j' g_{1,i-1}\hat{\boldsymbol{\xi}}_i g_{1,i-1}^{-1} - g_{1,i-1}\hat{\boldsymbol{\xi}}_i g_{1,i-1}^{-1}\hat{\boldsymbol{\xi}}_j' \\ &= \hat{\boldsymbol{\xi}}_j'\hat{\boldsymbol{\xi}}_i' - \hat{\boldsymbol{\xi}}_i'\hat{\boldsymbol{\xi}}_j' \\ &= [\hat{\boldsymbol{\xi}}_j' \quad \hat{\boldsymbol{\xi}}_i'].\end{aligned}$$

Then we can obtain (13) with the $\vee$(vee) operator.

REFERENCES

[1] Y. Nakamura, H. Hanafusa, and T. Yoshikawa, "Task-priority based redundancy control of robot manipulators," *The International Journal of Robotics Research*, vol. 6, no. 2, pp. 3–15, 1987.

[2] N. Mansard, O. Khatib, and A. Kheddar, "A unified approach to integrate unilateral constraints in the stack of tasks," *Robotics, IEEE Transactions on*, vol. 25, no. 3, pp. 670–685, 2009.

[3] Y. Wang, F. Vina, Y. Karayiannidis, C. Smith, and P. Ögren, "Dual arm manipulation using constraint based programming," in *19th IFAC World Congress*, Cape Town, South Africa, August 2014.

[4] R. Ortega and M. W. Spong, "Adaptive motion control of rigid robots: A tutorial," *Automatica*, vol. 25, no. 6, pp. 877–888, 1989.

[5] D. Bristow, M. Tharayil, A. G. Alleyne, *et al.*, "A survey of iterative learning control," *Control Systems, IEEE*, vol. 26, no. 3, pp. 96–114, 2006.

[6] J. De Schutter, T. De Laet, J. Rutgeerts, W. Decré, R. Smits, E. Aertbeliën, K. Claes, and H. Bruyninckx, "Constraint-based task specification and estimation for sensor-based robot systems in the presence of geometric uncertainty," *The International Journal of Robotics Research*, vol. 26, no. 5, pp. 433–455, 2007.

[7] H. Zghal, R. Dubey, and J. Euler, "Efficient gradient projection optimization for manipulators with multiple degrees of redundancy," in *Robotics and Automation, 1990. Proceedings., 1990 IEEE International Conference on*. IEEE, 1990, pp. 1006–1011.

[8] L. Sciavicco and B. Siciliano, "A solution algorithm to the inverse kinematic problem for redundant manipulators," *Robotics and Automation, IEEE Journal of*, vol. 4, no. 4, pp. 403–410, 1988.

[9] D. Oetomo and M. H. Ang Jr, "Singularity robust algorithm in serial manipulators," *Robotics and Computer-Integrated Manufacturing*, vol. 25, no. 1, pp. 122–134, 2009.

[10] S. Chiaverini, "Singularity-robust task-priority redundancy resolution for real-time kinematic control of robot manipulators," *Robotics and Automation, IEEE Transactions on*, vol. 13, no. 3, pp. 398–410, 1997.

[11] N. Van Der Aa, H. Ter Morsche, and R. Mattheij, "Computation of eigenvalue and eigenvector derivatives for a general complex-valued eigensystem," *Electronic Journal of Linear Algebra*, vol. 16, no. 1, pp. 300–314, 2007.

[12] R. M. Murray, Z. Li, S. S. Sastry, and S. S. Sastry, *A mathematical introduction to robotic manipulation*. CRC press, 1994.

[13] S. Chiaverini, B. Siciliano, and O. Egeland, "Review of the damped least-squares inverse kinematics with experiments on an industrial robot manipulator," *Control Systems Technology, IEEE Transactions on*, vol. 2, no. 2, pp. 123–134, 1994.

[14] G. Antonelli, "Stability analysis for prioritized closed-loop inverse kinematic algorithms for redundant robotic systems," *Robotics, IEEE Transactions on*, vol. 25, no. 5, pp. 985–994, 2009.

[15] P. Falco and C. Natale, "On the stability of closed-loop inverse kinematics algorithms for redundant robots," *Robotics, IEEE Transactions on*, vol. 27, no. 4, pp. 780–784, 2011.

[16] C. C. Cheah, M. Hirano, S. Kawamura, and S. Arimoto, "Approximate jacobian control for robots with uncertain kinematics and dynamics," *Robotics and Automation, IEEE Transactions on*, vol. 19, no. 4, pp. 692–702, 2003.

[17] Y. Wang, C. Smith, Y. Karayiannidis, and P. Ögren, "Cooperative control of a serial-to-parallel structure using a virtual kinematic chain in a mobile dual-arm manipulation application," in *IEEE/RSJ International Conference on Intelligent Robots and Systems*, Congress center Hamburg, Germany, Sepetember 2015.

[18] N. Likar, B. Nemec, and L. Žlajpah, "Virtual mechanism approach for dual-arm manipulation," *Robotica*, pp. 1–16, 2013.

[19] E. Malis and P. Rives, "Robustness of image-based visual servoing with respect to depth distribution errors," in *Robotics and Automation, 2003. Proceedings. ICRA'03. IEEE International Conference on*, vol. 1. IEEE, 2003, pp. 1056–1061.

[20] A. Muller, "Closed form expressions for the sensitivity of kinematic dexterity measures to posture changing and geometric variations," in *Robotics and Automation (ICRA), 2014 IEEE International Conference on*, May 2014, pp. 4831–4836.

[21] F. Chen, Z. Chen, Z. Liu, L. Xiang, and Z. Yuan, "Decentralized formation control of mobile agents: a unified framework," *Physica A: Statistical Mechanics and its Applications*, vol. 387, no. 19, pp. 4917–4926, 2008.

[22] R. E. Moore, R. B. Kearfott, and M. J. Cloud, *Introduction to interval analysis*. Siam, 2009.

[23] M. R. Pac, M. Rakotondrabe, S. Khadraoui, D. O. Popa, and P. Lutz, "Guaranteed manipulator precision via interval analysis of inverse kinematics," in *ASME 2013 International Design Engineering Technical Conferences and Computers and Information in Engineering Conference*. American Society of Mechanical Engineers, 2013, pp. V001T09A017–V001T09A017.

[24] F. C. Park, "Computational aspects of the product-of-exponentials formula for robot kinematics," *Automatic Control, IEEE Transactions on*, vol. 39, no. 3, pp. 643–647, 1994.